Available online at www.sciencedirect.com
SCIENCE DIRECT
Journal of Molecular Catalysis A: Chemical 246 (2006) 33–38
JOURNAL OF MOLECULAR CATALYSIS A: CHEMICAL
www.elsevier.com/locate/molcata

Direct decomposition of nitric oxide on alumina-modified amorphous and mesoporous silica-supported palladium catalysts

Julia María Díaz Cónsul [a], Carlos Alexandre Peralta [a], Edilson Valmir Benvenutti [a], Juan A.C. Ruiz [b], Heloise O. Pastore [b], Ione Maluf Baibich [a,*]

[a] *Instituto de Química, Universidade Federal do Rio Grande do Sul, CP 15003, 91501-970, Porto Alegre, RS, Brazil*
[b] *Instituto de Química, Universidade Estadual de Campinas, CP 6154, 13083-970, Campinas, SP, Brazil*

Received 26 August 2005; received in revised form 7 October 2005; accepted 10 October 2005
Available online 21 November 2005

Abstract

Palladium catalysts supported on SiO_2, MCM-41, [Al]-MCM-41 and on Al_2O_3-thin-layer- modified SiO_2 and MCM-41 were investigated for the direct decomposition of nitric oxide. The catalysts were characterized by X-ray diffraction, BET, SEM, UV-DRS and hydrogen chemisorption. All the catalysts studied were active in the NO decomposition reaction.

Keywords: NOx; MCM-41; Pd catalyst; NO decomposition

1. Introduction

The recently discovered mesoporous molecular sieve MCM-41 [1] has attracted considerable interest from researchers in the fields of materials science, catalysis, adsorption and other relevant areas [2–7].

This new member of the molecular sieve family shows a regular hexagonal array of uniform pores with pore opening dimensions between 1.5 and 10 nm [1]. As a consequence of their high thermal stability, high BET surface areas and large pore volumes, these materials could be considered to be excellent supports for metals in catalytic systems.

In addition, some papers dealing with the possibility of modifying the hydroxyl-rich surfaces by grafting alkoxides have been published recently [8–10], the surface coverage degree can be tuned by controlling the amount of metal alkoxide. Dispersing metal oxides, such as Al_2O_3 or ZrO_2, onto the inner pore surfaces can greatly improve the thermal stability [6].

As well as grafting or dispersing metals on the surface of mesoporous molecular sieves, metals can also be incorporated in the framework of the MCM-41. Aluminum can be introduced in the structure of these materials [11] generating a change in charge distribution that will be compensated by different cations [12]. In this way, new families (aluminosilicates, titanosilicates, germanosilicates, ferrisilicates, etc.) are obtained by the incorporation or substitution of cations in the structure, rendering these systems very interesting due to the presence of new active centers with redox properties or different acid strengths. The introduction of carefully selected metal ions can help tune catalyst activities and selectivities [13].

Therefore, mesoporous silica MCM-41 molecular sieves containing Zn and Al ions ([Zn]-MCM-41 and [Al]-MCM-41) were found to be effective in the alkylation of alkyl aromatics [11]. Chen and Lu [12] reported high catalytic activity for mesoporous vanadosilicate ([V]-MCM-41) in the oxidation of benzene. A MCM-41-supported palladium catalyst was used for aromatic hydrogenation [2,14,15] and liquid-phase hydrogenation [16]. Additionally, Long and Yang [3,17,18] reported that Cu^{2+}-, Rh^{2+}- and Fe^{3+}-exchanged [Al]-MCM-41 are effective catalysts for the selective catalytic reduction of nitric oxide with ethylene, propylene and NH_3, respectively. The same authors were the first to report the use of Pt-supported MCM-41 mesoporous sieves for the selective catalytic reduction of NO by hydrocarbons in the presence of oxygen. High activity for NO reduction was obtained when C_2H_4 or C_3H_6 were used as the reductants. The Pt/MCM-41 catalysts displayed good stability with respect to resistance to H_2O and SO_2. This property has been noted

* Corresponding author. Tel.: +55 51 33166304; fax: +55 51 33167304.
E-mail address: ione@iq.ufrgs.br (I.M. Baibich).

1381-1169/$ – see front matter © 2005 Elsevier B.V. All rights reserved.
doi:10.1016/j.molcata.2005.10.011

previously in the NO reduction reaction with hydrocarbons [19].

The direct catalytic decomposition of nitric oxide has been considered to be the best technique for NO removal from exhaust streams because nitrogen monoxide is thermodynamically unstable relative to N_2 and O_2 at low temperatures (between 20 and 700 °C). The development of an effective catalyst for direct NO decomposition would eliminate the use of reducing agents, significantly simplifying the NO removal process and decreasing the cost of NO control from the exhaust of various combustion processes [20,21].

The Cu-ZSM-5 catalyst has shown the highest activity for the direct decomposition of NO [22], however, the narrow temperature operation window, its rapid deactivation by water and susceptibility to SO_2 poisoning severely limit its practical use.

In previous works we have studied the performance of mono and bimetallic Pd catalysts supported on alumina and NaY zeolites [23–27].

In the present study, we compare the properties of palladium catalysts supported on SiO_2, siliceous MCM-41 and [Al]-MCM-41. SiO_2 and MCM-41 were also used as supports after modification with Al_2O_3 thin layers. These catalysts were characterized by powder X-ray diffraction (XRD), porosimetry (BET surface areas), scanning electron microscopy (SEM), diffuse reflectance UV spectroscopy (UV-DRS), hydrogen sorption and were finally tested in the direct decomposition of nitric oxide.

2. Experimental

2.1. Synthesis of MCM-41 [28]

Reaction mixtures were prepared by dissolving the required amount of sodium silicate (Nuclear, $Na_2SiO_3{\cdot}5H_2O$) in distilled water to give a 1.5 mol L^{-1} solution. To this clear solution, was added an aqueous suspension of cetyltrimethylammonium bromide (CTABr) (10.11 g of CTABr in 20.5 mL of water) aged for 24 h at room temperature. The mixture was stirred and the pH was slowly lowered from 13.40–13.60 to 10.80 by the addition of concentrated acetic acid. The suspension was then stirred for 4 h at 74–76 °C. The final gel composition was: SiO_2:Na_2O:0.25$(CTA)_2O$:0.5HBr:100H_2O. The reaction mixture was transferred to a Teflon-lined stainless steel autoclave and placed in a pre-heated oven at 150 °C, for a period of 66 h. After the hydrothermal treatment the samples were filtered and thoroughly washed with distilled water. The solids were air dried and sieved to 0.106 mm. To eliminate the organic part of these materials, a solvent extraction was performed in a Soxhlet system with 0.30 mol L^{-1} HCl solution in 50/50 ethanol/heptane, at 90 °C, over a period of 40 h. The samples were also calcinated by heating from room temperature to 500 °C at a rate of 5 K min^{-1}, under dry argon and then maintaining at that temperature for 20 h under dry oxygen [28].

For the [Al]-MCM-41 preparation, aluminum isopropoxide ($Al[OCH(CH_3)_2]_3$, 98+% Alfa Aesar) was added to the sodium silicate solution prior to the addition of the aqueous suspension of CTABr and the reaction performed as explained above. Throughout this work, the silica MCM-41 and the aluminosilicate MCM-41 are going to be referred to as MCM-41 and [Al]-MCM-41, respectively.

2.2. Modification of the support surfaces by the grafting reaction of a Al_2O_3 thin layer

Aluminum oxide was immobilized either on the supports by immersing 10 g of silica gel (Merck) or MCM-41 (synthesized as explained above), previously heated under vacuum at 150 °C for 8 h, in 50 mL of a 0.14 mol L^{-1} solution of aluminum isopropoxide in dry toluene. The mixture was heated at reflux temperature under an argon atmosphere for 24 h with mechanical stirring. The resulting solid was filtered under an inert atmosphere in a Schlenk apparatus and washed with warm toluene, ethanol and diethyl ether. The remaining solvent was removed under vacuum at 110 °C. In order to promote the Al–O–R bond hydrolysis, the modified supports were immersed in deionized water for 4 h, at room temperature. The mixture was filtered, washed with water and finally dried under vacuum at 120 °C [9]. The grafting reaction was repeated twice to obtain an Al_2O_3 monolayer on the silica gel and on the MCM-41 surfaces [10]. These samples were referred to as I Al_2O_3/MCM-41 (1% Al), II Al_2O_3/MCM-41 (3% Al) and III Al_2O_3/MCM-41 (5% Al), respectively. Pd was supported on the III Al_2O_3/MCM-41 sample.

2.3. Pd incorporation

The palladium catalysts were prepared by impregnation of the support (SiO_2, Al_2O_3/SiO_2 or III Al_2O_3/MCM-41) with a toluene solution of palladium acetylacetonate (8×10^{-3} g Pd mL^{-1}). The support was previously dried and activated at 450 °C in air for 3 h followed by another hour at the same temperature under vacuum. The solid (2 g) and the solution (7.5 mL) were left in contact for 24 h at room temperature. The liquid was removed; the solid was dried under vacuum, calcinated in air at 200 °C for 2 h and finally reduced in hydrogen under the same conditions. The palladium metal loading was adjusted in the synthesis to be 1 wt.%.

For the preparation of MCM-41 and Al-MCM-41 supported catalysts, palladium (II) acetate (98%) dissolved in acetone was transferred to an acetone suspension of the molecular sieves and the mixture was stirred for 6 h and evacuated until the excess of acetone was eliminated. After drying at 110 °C, the sample was heated at 500 °C at a rate of 5 °C min^{-1} for 4 h, under a flow of oxygen.

2.4. Catalysts characterization

MCM-41 samples were analyzed by powder X-ray diffraction (Shimadzu, XRD 6000), using Cu Kα radiation (λ = 1.5406 Å). The diffractometer was operated at 40 kV, 30 mA with a scan rate of 2° min^{-1} and a count time of 0.6 s. XRD patterns were recorded in the range of 1.4–50° (2θ).

For the scanning electron microscopy (SEM) analysis, the samples were dried at 100 °C for 2 h and coated with gold before the experiment. Samples were observed using a Jeol model

JSM 5800 scanning electron microscope, with 20 kV and 60,000 times of magnification.

The specific surface area of the solid previously degassed at 200 °C, under vacuum, was determined by BET (Brunauer, Emmett and Teller) multipoint technique on a ASAP 2010, micromeritics apparatus, using nitrogen as probe. The mesopore size distribution was obtained using BJH (Barret, Joyner and Halenda) method.

UV-diffuse reflectance spectra (DRS) of samples were recorded in the 200–800 nm range with a Cary 500 spectrophotometer, using $BaSO_4$ as a reference. The references for the experiments were the catalysts supports.

The palladium dispersion was determined by a hydrogen chemisorption method. The samples were pre-heated at 150 °C (10 °C min^{-1}) in flowing Ar (30 mL min^{-1}) for 0.5 h. They were then reduced at 300 °C (10 °C min^{-1}) under a flow of 1.74% H_2/Ar (30 mL min^{-1}). Following reduction, the samples were purged with Ar for 1 h at 300 °C and cooled to 70 °C (adsorption temperature) for hydrogen chemisorption using the dynamic method.

2.5. Catalytic activity

Catalytic experiments with NO were carried out in a fixed-bed quartz reactor. Prior to reaction, the catalysts were reduced in situ at 300 °C for 4 h. The NO decomposition reaction was studied as a function of time at 450 °C, using a feed mixture containing 500 ppm of NO in an argon background. The flow rate was adjusted to 120 cm^3 min^{-1} and the space velocity was 30,000 h^{-1}. The effluent gases were analyzed by a FTIR MB100-BOMEM spectrometer equipped with a multiple reflection gas cell (7.0 m path length and 2.1 L volume). The NO, NO_2 and N_2O stretching bands at 1955–1790 cm^{-1}, 1658–1565 cm^{-1} and 2266–2159 cm^{-1} respectively, were monitored. In order to calculate the NO conversions from the IR data, a method using the measured absorbance values [29] was used to determine the NO concentration at the entrance of the gas IR cell (reactor exit).

3. Results and discussion

Fig. 1 shows the X-ray diffraction patterns of the samples prepared in this work. Curve a in Fig. 1A displays the characteristic diffractogram for MCM-41. It is composed of one intense signal at low angles (2.40° 2θ), followed by two less intense ones, at 3.96° and 4.53° 2θ, corresponding to the (1 0 0), (1 1 0) and (2 0 0) diffractions, respectively, typical of a hexagonal array of parallel pores. In curves b, c and d (Fig. 1A) as the load of Al_2O_3 increases, there is a decrease in the overall diffractogram intensity, probably because of the different scattering properties of the Al_2O_3 layers, however the profiles indicate that the structure of MCM-41 is maintained during all these processes. The diminished total intensity was accompanied by a decreased intensity of the signals corresponding to the (1 1 0) and (2 0 0) in relation to the (1 0 0). This effect suggests that the MCM-41 structure became less ordered with the increased alumina layers concentration. The inclusion of palladium atoms did not further disturb either the relative organization of pores as the intensity of the (1 1 0) and (2 0 0) diffractions are not diminished, or the overall scattering properties of the solid (Fig. 1A, curve e). Fig. 1B shows the diffractograms of samples Pd/[Al]-MCM-41 (curve a), Pd/MCM-41 (curve b) and Pd/III-Al_2O_3-MCM-41 (curve c) after use in the catalytic reaction of NO decomposition. It is clear that the catalytic reaction does not provoke structure degradation or collapse; a peak at approximately 40.1° 2θ in these diffractograms indicates the presence of Pd in the cubic form [30]. It is interesting to note that the PdO in the tetragonal phase, present in the virgin catalyst (not shown), transforms itself into the cubic form during the reaction.

Typical SEM micrographs of SiO_2 and of MCM-41 particles are shown in Fig. 2. As it is observed, SiO_2 presents a more

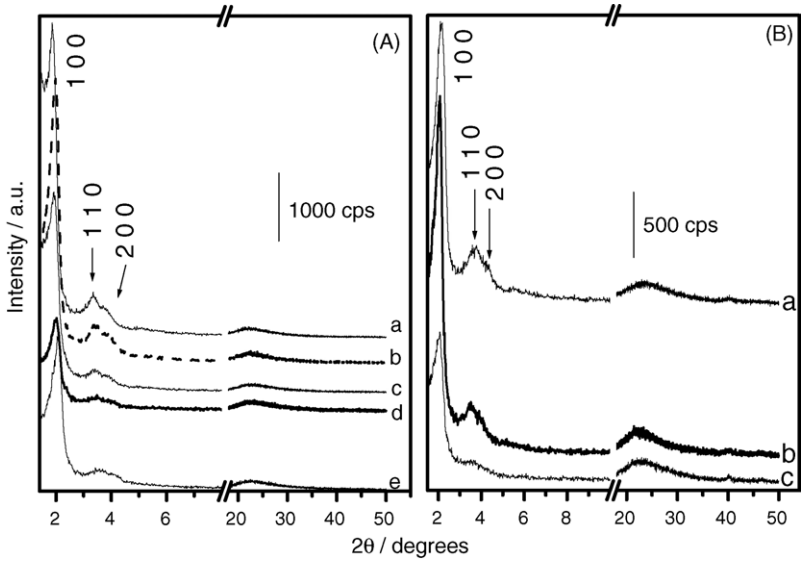

Fig. 1. Powder X-ray diffractograms of (A): (a) MCM-41, (b) I Al_2O_3/MCM-41, (c) II Al_2O_3/MCM-41, (d) III Al_2O_3/MCM-41 and (e) Pd/III-Al_2O_3/MCM-41; (B): catalysts after the reaction (a) Pd/[Al]-MCM-41, (b) Pd/MCM-41 and (c) Pd/III-Al_2O_3/MCM-41.

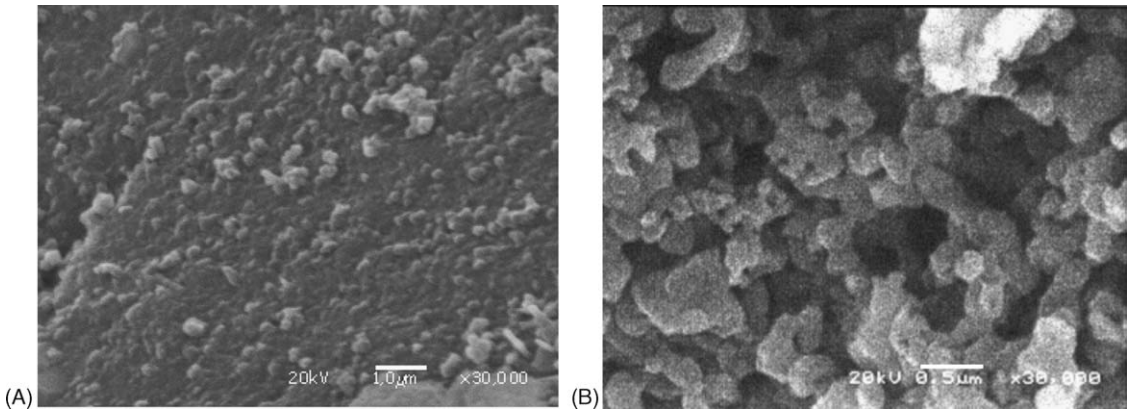

Fig. 2. Scanning electron microscopy images of (A) III Al_2O_3/SiO_2 and (B) III Al_2O_3/MCM-41.

compact inhomogeneous morphology characteristic of amorphous materials whereas the MCM-41 morphology is more regular, composed of independent and sintered hexagonal particles.

The impregnation of Pd or Pd/Al_2O_3 onto the amorphous silica surface does not change the surface area or pore volume of the support whereas the same treatment of the MCM-41 may incur important changes. Table 1 shows that on amorphous SiO_2 the total variation of surface area is in the order of 2% when both Pd and the thin Al_2O_3 film are present. For the mesoporous supports, it is possible to observe that the formation of the Al_2O_3 film causes a decrease of approximately 10% of the total surface area; if this cannot be considered strictly different, the presence of Pd and an alumina film simultaneously causes almost a 20% decrease in surface area. This decrease is related with the fact that the formation of the Al_2O_3 film and subsequent palladium occlusion have taken space in the intrazeolite channels and thus decreased the total surface area.

The type of palladium sites created inside the pores and channels of these supports was revealed by UV reflectance spectra (UV-DRS) (Fig. 3). The curves showed three wide bands peaking at 285, 353 and at 460 nm. The bands at 285 and 353 nm are attributed to a metal-ligand charge transfer and the one at 460 nm to a d–d transition [31]. Palladium oxide occluded in silica, Fig. 3, curves a and b, showed more intense bands than the metal catalyst on the MCM-41 supports probably due to the larger size of the palladium particles in silica [32] as indicated by the lower palladium dispersion shown in Table 1. Also, in these cases, the presence of larger bands due to d–d transitions at 460 nm indicates that the pores of the amorphous silica do not impose any constraints to the growing particles.

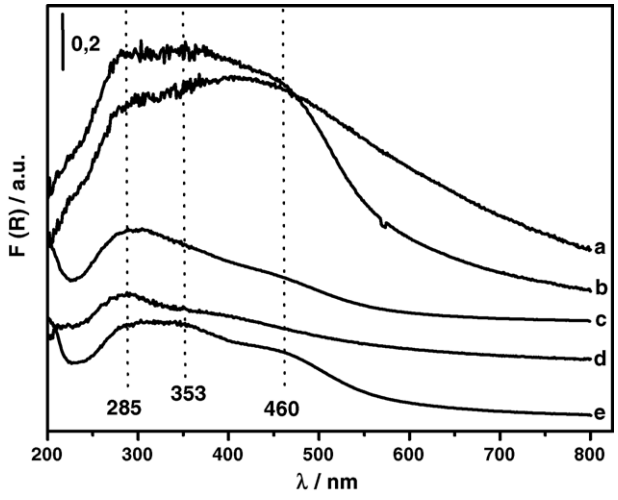

Fig. 3. Diffuse reflectance UV–vis spectra of Pd catalysts on the supports prepared in this work. (a) Pd/SiO_2, (b) $Pd/Al_2O_3/SiO_2$, (c) Pd/MCM-41, (d) Pd/Al_2O_3/MCM-41 and (e) Pd/[Al]-MCM-41.

A comparison of samples in Fig. 3, curves b and d, shows the influence of the organization of the catalyst support. The band at 353 nm is apparently absent or a lot weaker in the Pd/Al_2O_3/MCM-41 spectrum, indicating that larger Pd species are not present at all or are present in smaller quantities. The same effect is observed in comparing Pd/SiO_2 and Pd/MCM-41, curves a and c in Fig. 3, the effect of the presence of mesopores is easily seen as the band at higher wavelengths has increased in intensity, pointing to larger size Pd species.

The presence of an ion exchange site in the support is observed in the comparison between spectra in Fig. 3, curve c, for Pd supported on silica MCM-41 and curve e, for Pd supported on aluminosilicate MCM-41. The presence of a larger amount of connected species in the [Al]-MCM-41 is evidenced by the larger intensity of bands at 353 and 460 nm. The fact that some of the catalysts were prepared from palladium acetylacetonate and others from acetate did not seem to play a significant role in the determination of the Pd species formed in these supports.

The results of H_2 chemisorption (Table 1) shows that the use of MCM-41 as support leads to a higher Pd dispersion compared to the catalysts prepared on SiO_2. Additionally, it can be observed that the alumina layer on silica increases the Pd dispersion from 33 to 40% and on the MCM-41 significantly decreases the Pd dispersion, however to levels that still remain higher than on silica support.

As the metal dispersion was higher on MCM-41 support, the reduction of the catalyst on these supports was more difficult due to the stronger interaction of the smaller particles with these supports [33].

The catalytic tests are shown in Figs. 4 and 5. The catalysts prepared in this work display the same behavior; they are all active in the NO decomposition, as shown in Fig. 4. It is

Table 1
Palladium dispersions and pore structure parameters of the Pd catalysts

Catalysts	BET specific surface area ($m^2\ g^{-1}$)	Pore volume ($cm^3\ g^{-1}$)	Pore diameter (nm)	Pd dispersion (%)	Pd reducibility (%)	Pd loading (wt.%)
SiO_2	250	0.44		–	–	–
Pd/SiO_2	248	0.49		33	82	0.81
$Pd/Al_2O_3/SiO_2$	245	0.48		40	96	0.98
MCM-41	657	0.66	3.24	–	–	–
Pd/MCM-41	622	0.65	4.21	97		1.36
Pd/Al_2O_3/MCM-41	531	0.55	3.23	70	55	0.75
Pd/[Al]-MCM-41	717	0.77	4.30	82		1.43

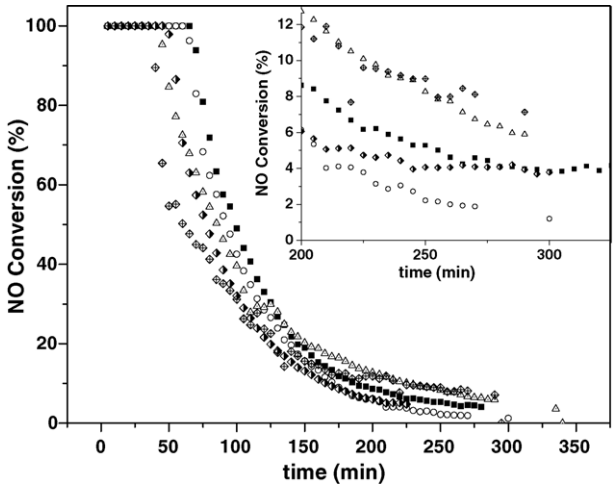

Fig. 4. NO conversion as a function of reaction time at 723 K. (■) Pd/SiO_2, (◯) $Pd/Al_2O_3/SiO_2$, (△) Pd/MCM-41, (◆) Pd/Al_2O_3/MCM-41 and (⊕) Pd/[Al]-MCM-41.

observed that Pd/SiO_2 and $Pd/Al_2O_3/SiO_2$ catalysts remain in 100% conversion for larger times than the other catalysts. As the conversion lowers, at around 100 min of reaction, the N_2O concentration starts to increase (Fig. 5). The curves are typical of Pd catalysts for the direct NO decomposition reaction. It is generally accepted that NO decomposition occurs on reduced metals [34], as oxygen is being formed and strongly adsorbed on the metal site the catalyst deactivates. Even so, if the results are compared with Pd-alumina catalysts studied before [24], despite different reaction conditions, the catalysts used in this work remained larger times at high conversion.

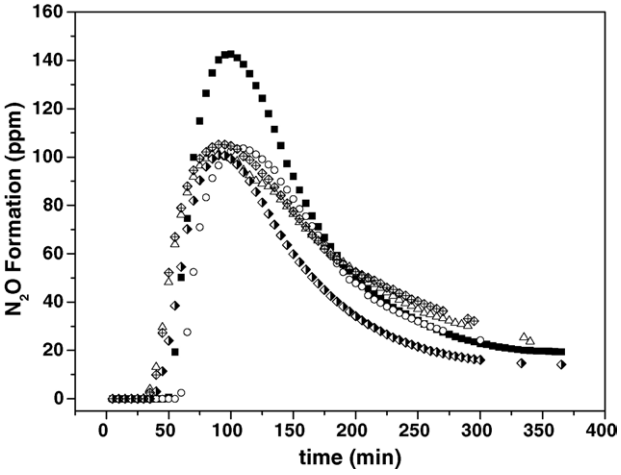

Fig. 5. N_2O formation as a function of time reaction at 723 K. (■) Pd/SiO_2, (◯) $Pd/Al_2O_3/SiO_2$, (△) Pd/MCM-41, (◆) Pd/Al_2O_3/MCM-41 and (⊕) Pd/[Al]-MCM-41.

Observing the activities at the low conversion region times of the catalysts based on MCM-41 (∼200 min reaction), one can see that Pd/Al-MCM-41 and Pd/MCM-41 have the best conversion values followed by Pd/Al_2O_3/MCM-41 (Fig. 4). This is in accord to the higher dispersion values found for the catalysts based on MCM-41 (Table 1). Examining the catalysts based on SiO_2 in the same figure, it is observed that at low conversion region times (∼200 min) Pd/SiO_2 catalyst presents a higher conversion than $Pd/Al_2O_3/SiO_2$ catalyst.

The Al_2O_3 film on both SiO_2 and MCM-41 seemed to lower the catalyst activity. On the other hand, when the aluminum is part of the structure (Pd/[Al]-MCM-41) the catalyst presented analogous activity to that of Pd/MCM-41. Furthermore, in Fig. 5 it can be seen that the less selective catalyst (the one that produces more N_2O) is Pd/SiO_2.

In all catalysts studied no significant NO_2 formation was detected.

4. Conclusions

Pd-supported SiO_2, MCM-41 and [Al]-MCM-41 were prepared either by direct grafting of palladium on the support or by impregnation onto the alumina-modified solids. X-ray diffraction showed that the structure of the mesoporous supports was not destroyed by the impregnation nor by the catalytic tests, a signal at approximately 40° 2θ was found in the X-ray diffractogram of the catalysts and indicated the formation of a cubic Pd phase after the catalytic reaction. The UV–vis reflectance spectra (UV-DRS) of the catalyst suggested that the types of sites found for palladium depended mainly on the nature of the support and not on the metal source. The better dispersed metal phase was observed in the catalyst-supported on MCM-41. The alumina thin film modification on the supports did not improve the performance of the catalysts. On the contrary, there was a decrease in activity when the film was present. Therefore, when Al was present in the structure it did not inhibit the catalyst activity.

Acknowledgements

The authors acknowledge the financial support provided by CNPq (Brazil), FAPERGS (Brazil), COPESUL (Brazil) and to

Dr. John Spencer (John Black foundation, England) for proof reading this article.

References

[1] C.T. Kresge, M.E. Leonowicz, W.J. Roth, J.C. Vartuli, J.S. Beck, Nature 357 (1992) 710.
[2] K. Okumura, H. Tokai, M. Niwa, Photon Factory Activity Report (2003) #20 Part B 2002.
[3] R.Q. Long, R.T. Yang, J. Phys. Chem. B 103 (1999) 2232.
[4] V.L. Zholobenko, D. Plant, A.J. Evans, S.M. Holmes, Micropor. Mesopor. Mater. 44–45 (2001) 793.
[5] M. Tiemann, M. Froba, Chem. Mater. 13 (2001) 3211.
[6] K. Wan, Q. Liu, C. Zhang, Mater. Lett. 57 (2003) 3839.
[7] F. Kleitz, W. Schmidt, F. Schüth, Micropor. Mesopor. Mater. 44–45 (2001) 95.
[8] P. Iengo, M. Di Serio, A. Sorrentino, V. Solinas, E. Santacesaria, Appl. Catal. A: Gen. 167 (1998) 85.
[9] S.T. Fujiwara, Y. Gushikem, R.V.S. Alfaya, Colloids Surf. A: Physicochem. Eng. Aspects 178 (2001) 135.
[10] J.M.D. Cónsul, I.M. Baibich, E.V. Benvenutti, Quím. Nova 28 (2005) 393.
[11] M. Selvaraj, A. Pandurangan, P.K. Sinha, Ind. Eng. Chem. Res. 43 (2004) 2399.
[12] Y.-W. Chen, Y.-H. Lu, Ind. Eng. Chem. Res. 38 (1999) 1893.
[13] N.C. Masson, H.O. Pastore, Micropor. Mesopor. Mater. 32 (2001) 224.
[14] V.L. Barrio, P.L. Arias, J.F. Cambra, M.B. Güemez, B. Pawelec, J.L.G. Fierro, Appl. Catal. A: Gen. 242 (2003) 17.
[15] J.N. Armor, Appl. Catal. A: Gen. 112 (1994) N21.
[16] J. Panpranot, K. Pattamakomsan, T.G. Goodwin Jr., P. Praserthdam, Catal. Commun. 5 (2004) 583.
[17] R.Q. Long, R.T. Yang, Ind. Eng. Chem. Res. 38 (1999) 873.
[18] R.T. Yang, T.J. Pinnavaia, W. Li, W. Zhang, J. Catal. 172 (1997) 488.
[19] R. Long, R. Yang, Catal. Lett. 52 (1998) 91.
[20] G.M. Tonetto, M.L. Ferreira, D.E. Damiani, J. Mol. Catal. A: Chem. 193 (2003) 121.
[21] S.S.C. Chuang, C.-D. Tan, J. Phys. Chem. 101 (1997) 3000.
[22] M. Iwamoto, H. Hamada, Catal. Today 10 (1991) 57.
[23] I.M. Baibich, J.H. dos Santos, V.C. da Silveira, C.E. Gigola, A.M. Sica, Can. J. Anal. Sci. Spectros. 43 (1998) 26.
[24] A.M. Sica, J.H. dos Santos, I.M. Baibich, C.E. Gigola, J. Mol. Catal. A: Chem. 137 (1999) 287.
[25] R.M.J. de Almeida, S.B.C. Pergher, C.E. Gigola, I.M. Baibich, Can. J. Anal. Sci. Spectros. 48 (2003) 21.
[26] A.M. Sica, I.M. Baibich, C.E. Gigola, J. Mol. Catal. A: Chem. 195 (2003) 225.
[27] S.B.C. Pergher, R.M. Dallago, R.C. Veses, C.E. Gigola, I.M. Baibich, J. Mol. Catal. A: Chem. 209 (2004) 107.
[28] H.O. Pastore, M. Munsignatti, D.R.S. Bittencourt, M. Rippel, Micropor. Mesopor. Mater. 32 (1999) 211.
[29] R.M. Dallago, J. Schifino, I.M. Baibich, R.C. Veses, Can. J. Anal. Sci. Spectros. 49 (2004) 78.
[30] P.O. Thevenin, A. Alcalde, L.J. Pettersson, S.G. Järås, J.L.G. Fierro, J. Catal. 215 (2003) 78.
[31] F.B. Noronha, D.A.G. Aranda, A.P. Ordine, M. Schmal, Catal. Today 57 (2000) 275.
[32] M. Lyubovsky, L. Pfefferle, Catal. Today 47 (1999) 29.
[33] R. Burch, J.P. Breen, F.C. Meunier, Appl. Catal. B: Environ. 1220 (2002) 1.
[34] S. Kawi, O. Alexeev, M. Shelef, B.C. Gates, J. Phys. Chem. 99 (1995) 6926.